Proceedings of The National Conference
On Undergraduate Research (NCUR) 2017
University of Memphis, TN
Memphis, Tennessee
April 6-8, 2017

Classification of Normal and Lesional Colon Tissue Using Fluorescence Excitation-Scanning Hyperspectral Imaging as A Method for Early Diagnosis of Colon Cancer

[1]Malvika Lall , [1]Joshua Deal
[1]Department of Chemical and Biomolecular Engineering, [2]Department of Pharmacology,
[3]Center for Lung Biology, [4]Department of Pathology, [5]Department of Surgery
University of South Alabama
Mobile, AL 36608, USA

Faculty Advisors: Dr. Shante Hill[4], Dr. Paul F. Rider[5], Dr. Carole W. Boudreaux[4],
Dr. Thomas C. Rich[2], Dr. Silas Leavesley[1,2,3]

Abstract

Colon cancer is the second leading cause of cancer death in the United States. The purpose of colorectal screening exams is the detection and diagnosis of lesions to help reduce the associated morbidity and mortality by identifying lesions early and accurately prior to advancement into cancer or tissue invasion. The objective of this study is to classify colon tissue into normal and lesional tissue by measuring spectral changes using Fluorescence Excitation-Scanning Hyperspectral Imaging. Fresh normal and colon cancer surgically resected tissue specimens were obtained in collaboration with the University of South Alabama Departments of Surgery and Pathology and prepared for scanning. All procedures were carried out in accordance with Institutional Review Board protocol # 13-120. Normal and cancerous tissue types were confirmed by histologic evaluation of H&E permanent sections and scanned by excitation scanning hyperspectral imaging using a novel microscope constructed at the University of South Alabama. At least three fields of view (FOV) were located on each specimen. MATLAB and ENVI were used for spectral correction and to extract the spectra from each region of interest. Spectral graphs for each region of interest for both lesional and normal tissue were generated and compared. Results comparing average spectra obtained from normal colon tissue showed homogeneity, as demonstrated by spectral images with similar peak wavelengths and shapes in all regions of interest within a FOV. However, in comparison the extracted spectra from colon cancer showed high heterogeneity with spectral images of varying peak wavelengths and shapes. Results from an automated classification using a Maximum Likelihood algorithm yielded high sensitivity (97.91) and high specificity (92.75) values, showing that there was a high probability that a cancerous pixel was correctly classified as cancerous and a high probability that a normal pixel was correctly classified as normal respectively. A high overall accuracy (94.99%) showed that most pixels were correctly classified. We conclude that fluorescence excitation-scanning hyperspectral imaging could detect differences in the spectral patterns of normal and lesional colon tissue which would allow for the classification of colon tissue into normal and lesional tissue types. This information could be used in the development of new methods for early diagnosis of colon cancer by translating the technology into a real-time endoscopic platform to classify tissues based on the spectral changes.

Keywords: Colon cancer, classification, spectral patterns

1. Introduction

Colon cancer is the second leading cause of cancer death in the United States. [8] The purpose of colorectal screening exams is early detection and diagnosis of lesions to help reduce the associated morbidity and mortality. [15] Most

colorectal cancers begin as a growth on the mucosa of the colon, which is the innermost layer of the wall of the colon. [22] This growth, known as a polyp can be noncancerous, precancerous, or cancerous. The potential of a polyp to become cancerous depends on its type, with adenomatous polyps having the potential to become malignant whereas hyperplastic polyps are not precancerous. [8] The most common colorectal cancers are adenocarcinomas with others including carcinoid tumors, stromal tumors, lymphomas, and sarcomas. Colon cancer is staged from 0 to IV with the 5-year colon cancer–specific survival decreasing from stage I to stage IV. [2], [15] Because most early lesions produce no discernible symptoms and are generally only found during a colonoscopy procedure, it is important that the screening procedure used is a method that provides early but yet accurate detection of colon cancer.

The gold-standard procedure for colorectal screening in the United States is traditional white light endoscopy. [8] However, the miss rates for lesions with this procedure have been shown to range from 0% to 20% with higher miss rates for flat and small (<5mm) lesions. [6], [16], [18], [19] In addition, alternative screening techniques including auto-fluorescence imaging, chromoendoscopy, and narrow band imaging, [8], [10], [11], [12], [23] have not shown significant improvements in detection sensitivity and specificity. [3], [7], [14]

A potential alternative technology is spectral imaging, which uses wavelength dependent reflectance and/or fluorescence properties of tissues to differentiate them. Different tissues have varying reflectance or fluorescence at different wavelengths and therefore can be distinguished based on their wavelength dependent signatures. [1], [13] The specificity of single wavelength fluorescence techniques, such as AFI, is low due to the inability to differentiate between fluorophores with similar peak emission wavelengths. However, hyperspectral imaging produces a spectral signature for every pixel in an image that can be used to estimate the molecular composition of the pixel. [3]

Traditionally, fluorescence hyperspectral imaging has been implemented through scanning of the emission spectrum, which results in a weak signal because the emitted light is filtered to a narrow band prior to detection. This limitation requires longer acquisition times to account for the diminished signal making emission scanning hyperspectral imaging an unsuitable method for time sensitive procedures such as video rate endoscopy. [4] A new spectral imaging method, hyperspectral imaging using fluorescence excitation scanning (HIFEX), allows detection of signals from all emitted light at a particular excitation wavelength and has been shown to increase the signal sensitivity by 10 to 30-fold compared to emission-scanning methods. [4] Hence, the new HIFEX technique allows for faster acquisition times and the possibility to be incorporated into real-time endoscopic procedures to identify tissue types based on spectral changes.

The goal of this study is to assess the potential of HIFEX microscopy to measure spectral changes that are indicative of molecular changes occurring in colorectal cancer when compared to adjacent normal tissue in resected colon tissue and to be able to classify colon tissue into normal and lesional tissue based on these spectral changes.

2. Materials and methods

2.1 Tissue Specimens

Fresh normal and colon cancer surgically resected tissue specimens were obtained in collaboration with the University of South Alabama Departments of Surgery and Pathology and confirmed by histologic evaluation of H&E permanent sections. All procedures were carried out in accordance with Institutional Review Board protocol # 13-120. Specimens were identified as HSI-1, HSI-2, etc., for each patient enrolled in the study.

2.2 Sample Preparation

Surgically resected tissue specimens were transported on an ice pack to the lab for imaging. Specimens were subdivided and placed on a coverslip mounted in an attafluor and wetted with PBS prior to imaging. Specimens were imaged using a novel hyperspectral imaging fluorescence excitation-scanning (HIFEX) microscope constructed at the University of South Alabama and described below.

2.3 Microscope, Equipment and Hyperspectral Excitation-Scanning Image Acquisition

The base imaging platform was an inverted fluorescence microscope (TE2000-U, Nikon Instruments) with a 20x objective lens (10x/.25 Ph1 ADL ∞/1.2 WD 6.2, Nikon Instruments). Illumination was provided by a 300W Xenon arc lamp (TITAN 300ST-K, Sunoptics Technologies). Illumination was filtered through a thin-film tunable filter

system (Sutter, VF5) containing five separate tunable filters (Semrock, VersaChrome filters). This filter system is described in detail by Favreau et al 2014. [4] Filtered excitation light was directed to the microscope using a liquid light guide and was reflected off of a 555nm long-pass dichroic beam splitter through the microscope objective to the specimen. Fluorescence emission was detected through a 561nm long pass emission filter. Images were acquired using an electron multiplied charge-coupled device (CCD) camera (Rolera EM-C 2 EMCCD, QImaging Corp.). At least three fields of view (FOV) were acquired for each tissue specimen. The fluorescence excitation was scanned through each excitation wavelength sequentially using wavelength ranges from 340- 520nm, in 5nm increments, and the long-pass fluorescence emission signal was detected at each excitation wavelength. Figure 1 shows a schematic light path used for excitation-scanning, and Figure 2 shows the microscope setup.

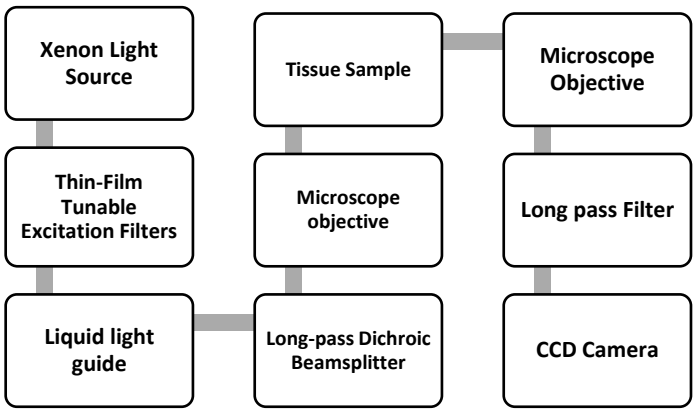

Figure 1: Excitation scanning light path

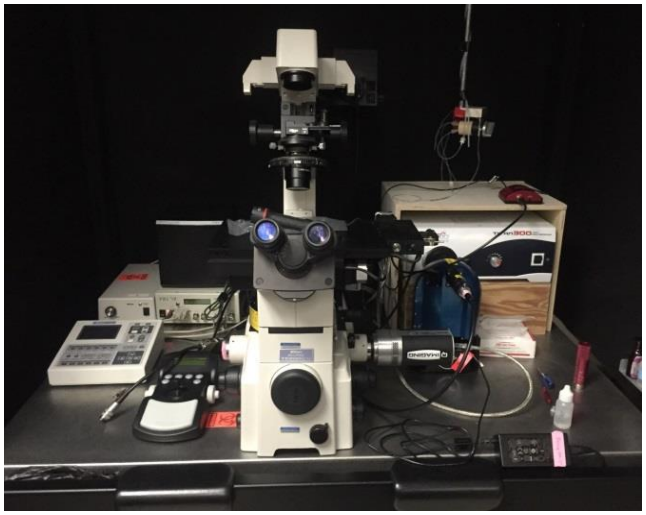

Figure 2: HIFEX Microscope setup for excitation scanning.

2.4 Spectral Correction

A spectral correction factor to account for differences because of wavelength-dependent illumination or transmission was used. [25] A background spectrum was acquired from each specimen for use in the flat spectral correction process. For each tissue, one FOV was acquired in which some of the region was outside of the tissue. With the use of MATLAB and ENVI, the spectrum of this region was used as a background spectrum for correcting all of the spectral image data acquired from the specimen. Correction of the images also aided in choosing certain regions of interest (ROI). Figures 3 and 4 demonstrate the spectral correction in normal and lesional tissue respectively.

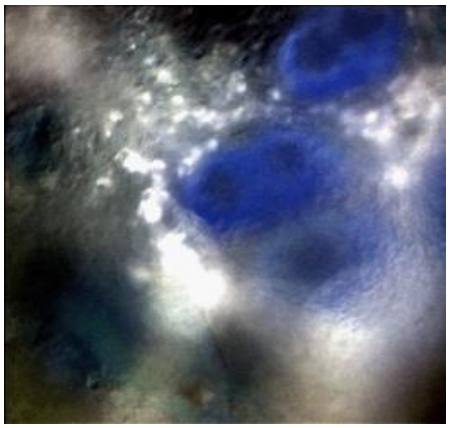

Figure 3: Correction of Image HSI-1NormalTissue FOV2

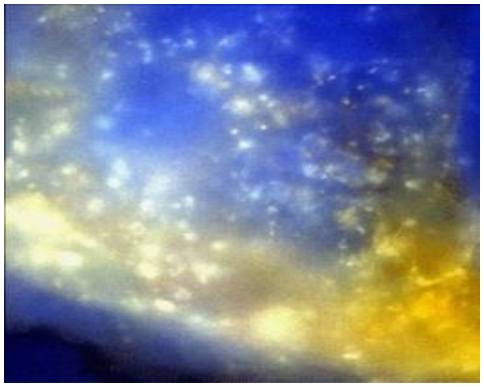

Figure 4: Correction of Image HSI-1 Lesional Tissue FOV3

2.5 Spectral Image Collection and Analysis

2.5.1 collecting background spectrum

A background spectrum was measured for each specimen and used during the spectral correction process. MATLAB (The MathWorks) and ENVI (ITT Visual Solutions Inc.) were used to determine the background spectrum. The first field of view (FOV1) for each specimen was always selected so as to acquire an image with the tissue comprising roughly 50% of the image and a blank region (background) comprising the other 50%. To measure the average background spectrum, a region of interest (ROI) was drawn in the background area (lacking tissue) using the ROI tool in ENVI, and the average spectrum of the background ROI was measured. The background spectrum was exported to Excel (Microsoft Corp.), transferred onto an excel file and saved as a text file. A custom MATLAB script was used to perform background subtraction and flat spectral correction. The spectrally-corrected image file was saved in band sequential (BSQ) format, with a corresponding text header file that allowed the corrected files to be opened in ENVI software. Spectra were then plotted and spectral differences assessed.

2.5.2 identifying structural features and extracting spectral data

The identification of structural features based on anatomical structures was done by the selected ROI method. Figure 5 shows lesional tissue in HSI-1 with various regions of interest indicated. In each ROI, the average intensity at each wavelength was calculated and the intensity data was extracted as the average spectrum. The regions were displayed with different colors for visualization. Spectral graphs were generated for each region of interest for normal and lesional tissue. These spectral graphs were compared to identify differences in spectral patterns between the two tissue types.

2.5.3 classification

ENVI software was used to classify images of normal and lesional tissues, using a supervised classification algorithm called Maximum Likelihood. After identifying the training regions, we identified the "truth" regions to assess the classification accuracy in identifying pixels as either normal or lesional. A confusion matrix was generated to display correctly classified pixels. Detection sensitivity, specificity, and accuracy were also calculated.

Figure 5: FOV3 HSI-1 Lesional tissue with identified Regions of Interest

3. Results

3.1 Normal Tissue Results

In general, normal tissues were observed to be spectrally homogeneous as the shapes of the spectra were similar for different regions of interest within the field of view and across multiple field of views for all three patients (Figures 6, 7, 8, 9 and 10). In figures 6 through 10, which are spectra of different regions of interest in the same field of view, the spectral patterns were all same within a particular FOV. This gives normal tissue the characterization of being homogeneous. One exception was patient 2 (HSI-2) FOV2 normal tissue shown in Figure 8, which showed a variance in one of the ROI spectra from the rest of the ROI's in that particular field of view. This was thought to be due to possible inclusion of a lesional area in the normal tissue sample or possible contamination.

3.2 Lesional Tissue Results

The lesional tissues were observed to be spectrally heterogeneous as the spectra for the different regions of interest were significantly different within a given field of view. Figures 11 through 16 demonstrate this heterogeneity. Each figure is a representation of the spectra of different regions of interest within a field of view in the lesional tissue. Peaks of various intensities occurred in different ROI areas in a field of view in the lesional tissue. These variations were not present in the normal tissue. Overall, the spectra for lesional tissues differed greatly from normal tissues which allowed the lesional tissues to be identified based on the heterogeneity of the spectral patterns.

3.3 Accuracy of Results

Supervised training algorithms were used to differentiate between normal and lesional tissue (Figure 17). Specificity and Sensitivity values calculated for the created spectra revealed a sensitivity of 97.91 and a specificity of 92.75 with a PPV of 91.19, NPV of 98.30 and a high overall accuracy of 94.99% (Figure18). These values of specificity and sensitivity indicate a high probability that a cancerous pixel will be correctly classified as cancer and a high probability that normal pixel will be correctly classified as normal, respectively.

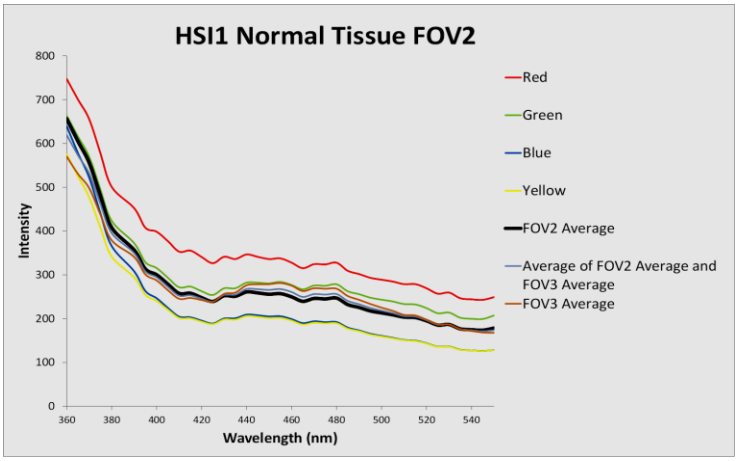

Figure 6**:** Normal tissue HSI-1 FOV2 with similar spectral patterns in all regions of interest in a single field of view. Each ROI is represented by a different color.

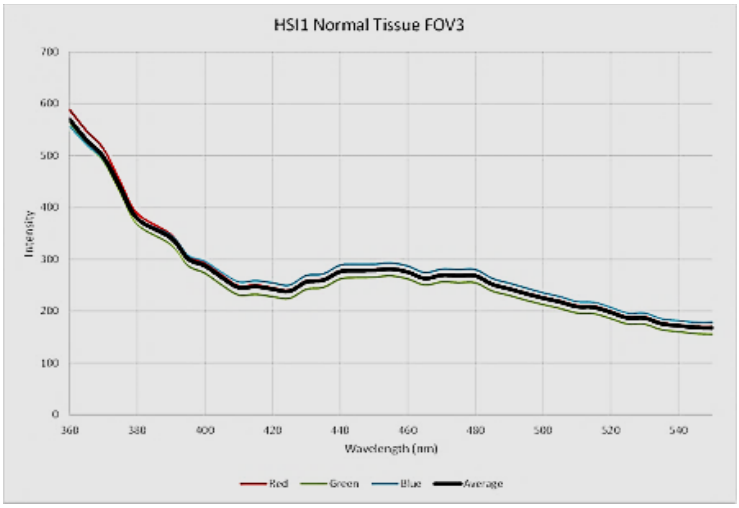

Figure 7: Normal tissue HSI-1 FOV3 with spectral patterns of all ROI's in a single field of view demonstrating a homogeneous pattern. Each ROI is represented by a different color.

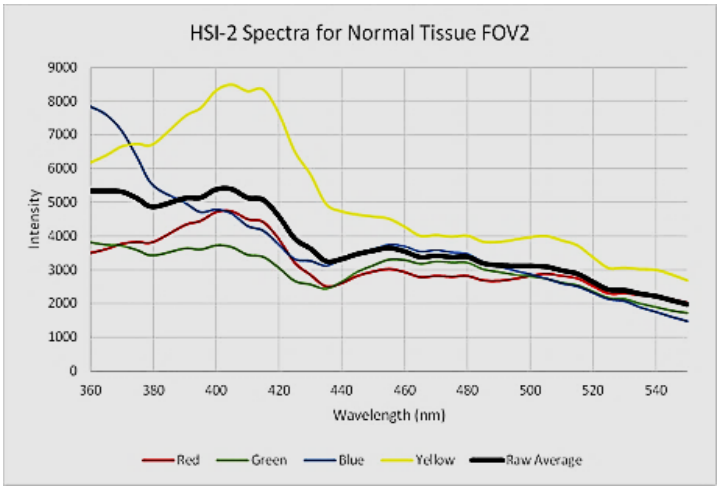

Figure 8: Normal tissue HSI-2 FOV2 with similar spectral patterns in all ROI's except one in a single field of view. This was an exception to the normal tissue homogeneous spectral pattern.

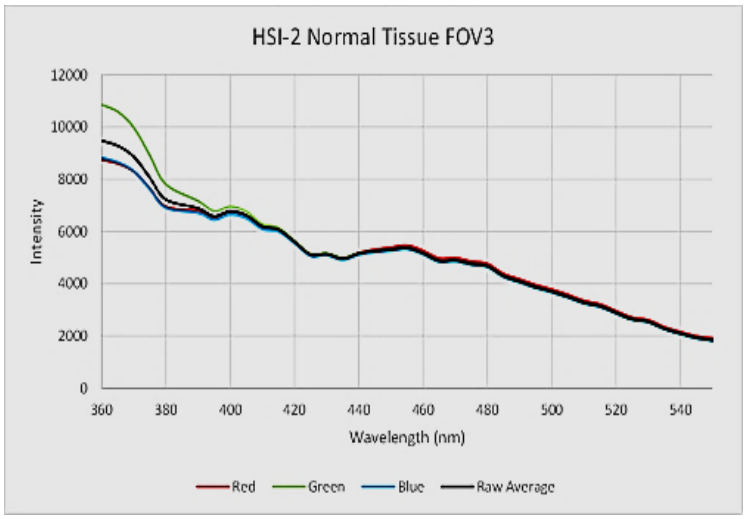

Figure 9: Normal tissue HSI-2 FOV3 with similar spectral patterns in all ROI's in a single field of view demonstrating homogeneity. Each ROI is represented by a different color.

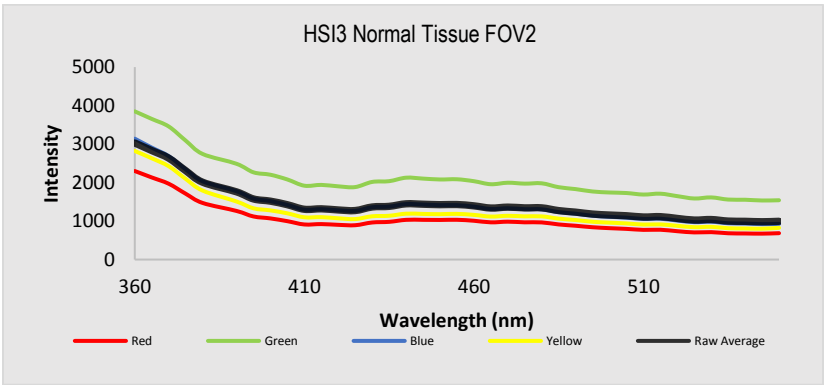

Figure 10: Normal tissue HSI-3 FOV2 with similar spectral patterns in all ROI's in a single field of view demonstrating homogeneity. Each ROI is represented by a different color.

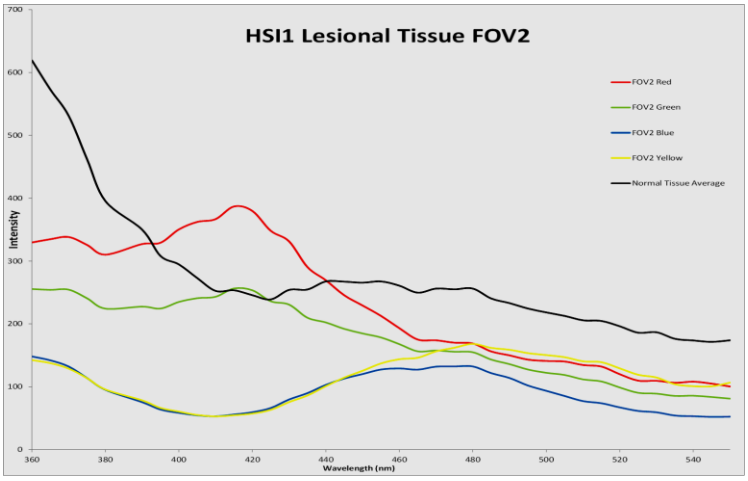

Figure 11: Lesional tissue HSI-1 FOV2 with heterogeneous spectral patterns in a single field of view. There are peaks of various intensities in the spectral patterns of different regions of interest within a field of view. Each ROI is represented by a different color.

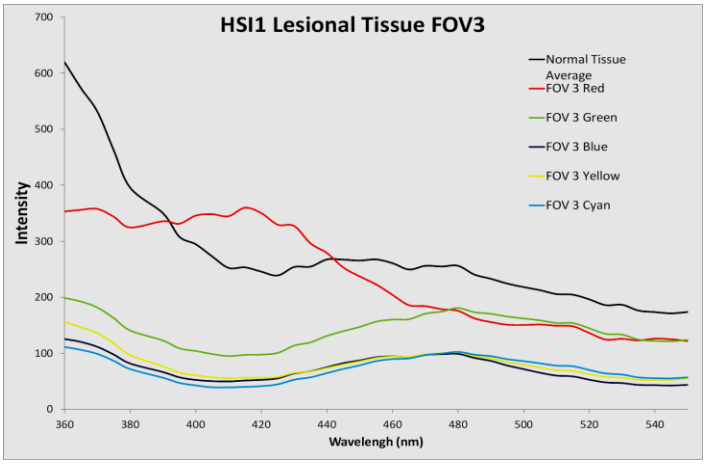

Figure 12: Lesional tissue HSI-1 FOV3 with heterogeneous spectral patterns with peaks of various intensities in a single field of view. Each ROI is represented by a different color.

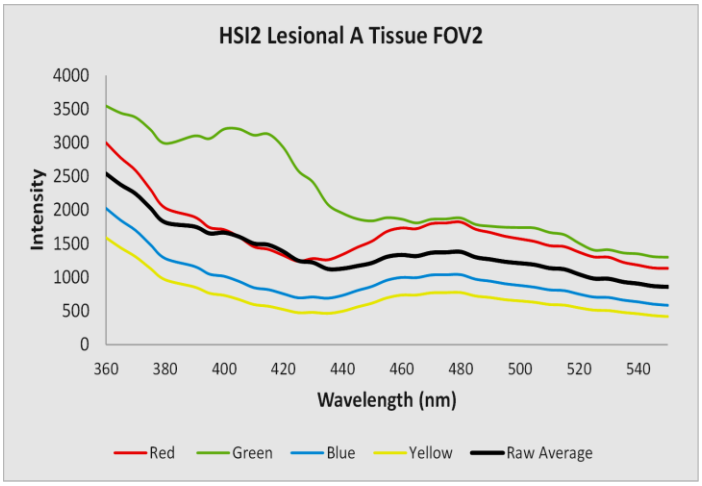

Figure 13: Lesional tissue HSI-2 FOV2 with heterogeneous spectral patterns of different regions of interest in a single field of view. Each ROI is represented by a different color.

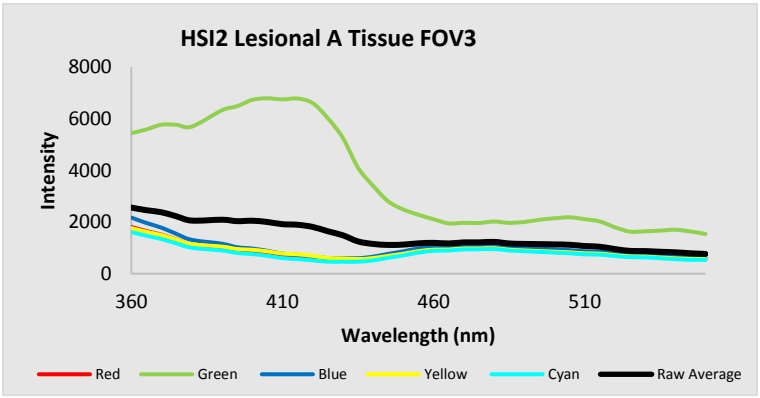

Figure 14: Lesional tissue HSI-2 FOV3 with heterogeneous spectral patterns of different regions of interest in a single field of view. Each ROI *is represented by a different color*.

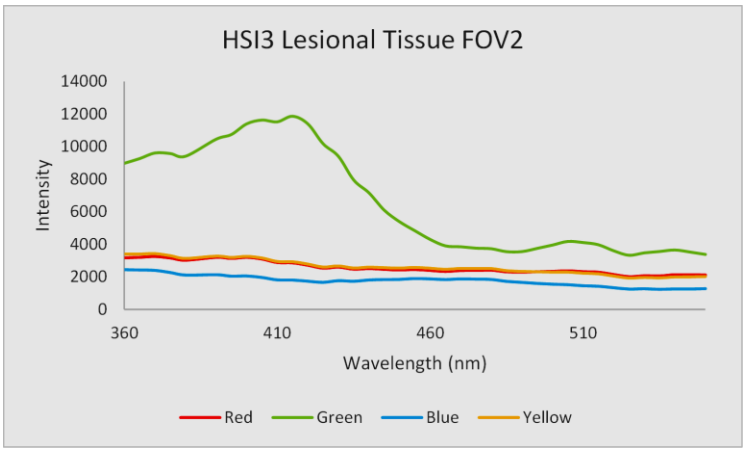

Figure 15: Lesional tissue HSI-3 FOV2 with heterogeneous spectral patterns of different regions of interest in a single field of view. Each ROI is represented by a different color.

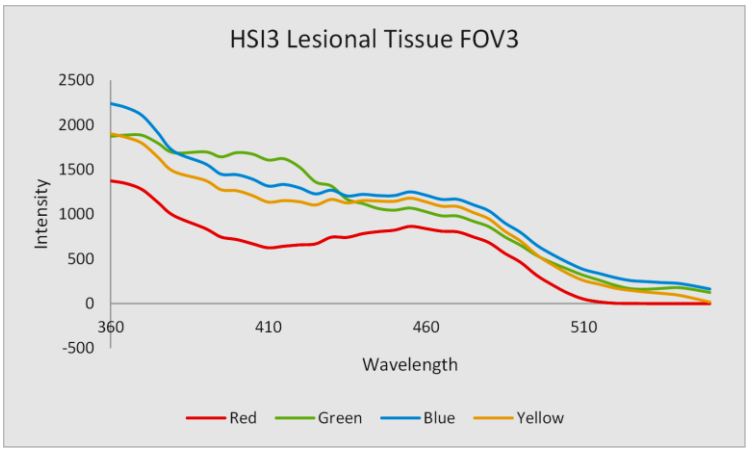

Figure 16: Lesional tissue HSI-3 FOV3 with heterogeneous spectral patterns of different regions of interest in a single field of view. Each ROI is represented by a different color.

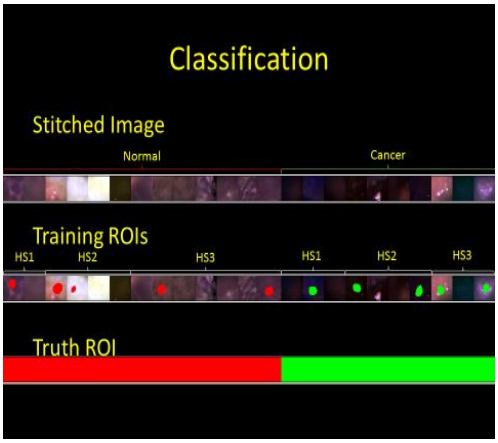

Figure 17: Creation of Training and truth regions. ENVI was used to create Training and Truth regions to help to classify the tissue into Normal and Lesional.

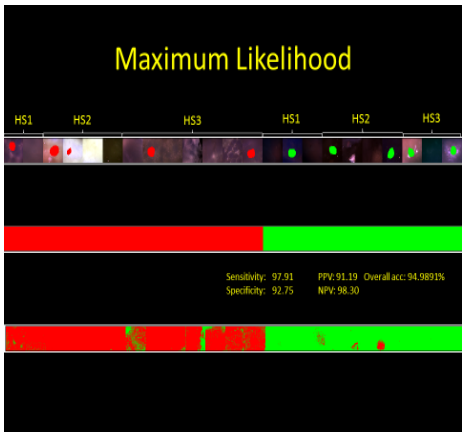

Figure 18: Maximum Likelihood. Classification of images were done using a supervised training algorithm called Maximum Likelihood. A confusion matrix was then used to determine sensitivity, specificity, and accuracy

4. Discussion

Hyperspectral fluorescence excitation-scanning imaging allowed classification of colon tissue into normal and lesional based on differences in the fluorescence excitation spectra for normal and cancerous tissues. When comparing average spectra for FOV2 and FOV3 in HS1-1 normal tissue, the spectra were very similar in peak wavelengths and intensities. Similar results were seen in the FOV's in HSI-2 and HSI-3 normal tissue. The spectra from each FOV from normal tissue in all 3 patients appeared similar and were classified as homogeneous. The lesional tissue had significantly different spectra compared to the normal tissue sample. The spectra showed peaks of various intensities that occurred over a range of peak wavelengths in the lesional tissue. These variations were not present in the normal tissue. The lesional tissue also presented varying spectra across different ROI's within a FOV and was, therefore, classified as having a heterogeneous appearance.

5. Conclusions

This study demonstrated that the fluorescence excitation spectral patterns of normal and lesional colon tissue were different and could be detected using fluorescence excitation-scanning hyperspectral imaging. This allowed for classification of colon tissue into normal and lesional. Normal tissue was characterized as spectrally homogeneous as the shape of the spectra were significantly similar for most ROI's within a FOV. By comparison, the lesional tissue was characterized as spectrally heterogeneous, as the spectra for different ROIs were significantly different within a FOV. Classification of tissues using a Maximum Likelihood algorithm resulted in a high accuracy as shown by the calculated high sensitivity and specificity. The future application of this study is based on the fact that hyperspectral fluorescence excitation-scanning may be capable of producing fast acquisition times and, therefore, can be incorporated into real-time endoscopic procedures to identify tissue types based on spectral changes.

6. Acknowledgements

The authors would like to acknowledge support from:
NIH grants UL1 TR001417 and P01 HL066299, The Abraham Mitchell Cancer Research Fund, and The University of Alabama at Birmingham Center for Clinical and Translational Science (CCTS).

7. References

1. Akbari H, Uto K, Kosugi Y, Kojima K, Tanaka N. Cancer detection using infrared hyperspectral imaging. Cancer Sci.102(4), 852-857 (2011).

2. American Joint Committee on Cancer. Colon and Rectum Cancer Staging. 7th Ed

3. Chiu H.M, Chang C.Y, Chen C.C, Lee Y.C, Wu M.S, Lin J.T, Shun C.T and Wang, H.P. A prospective comparative study of narrow-band imaging, chromoendoscopy, and conventional colonoscopy in the diagnosis of colorectal neoplasia. Gut 56, 373–379 (2007).

4. Favreau P. F, Hernandez C, Heaster T, Alvarez D.F, Rich T.C, Prabhat P and Leavesley S. Excitation-scanning hyperspectral imaging microscope. J. Biomed. Opt. 19, 046010–046010 (2014).

5. Favreau P. F, Hernandez C, Lindsey A.S, Alvarez D.F, Rich T.C, Prabhat P and Leavesley S. Thin-film tunable filters for hyperspectral fluorescence microscopy. J. Biomed. Opt. 19, 011017 (2014).

6. Hixson, L., Fennerty, M., Sampliner, R. & Garewal, H. Prospective blinded trial of the colonoscopic miss-rate of large colorectal polyps. Gastrointest. Endosc. 37, 125–127 (1991).

7. Ignjatovic, A., East, J.E., Guenther, T., Hoare, J., Morris, J., Ragunath, K., Shonde, A., Simmons, J., Suzuki, N., Thomas-Gibson, S. and Saunders, B.P. What is the most reliable imaging modality for small colonic polyp characterization? Study of white-light, autofluorescence, and narrow-band imaging. Xu, J., Murray, T. and Thun, M.J. Endoscopy 43, 94 (2011).

8. Jemal, A., Segal, R., Ward, E., Hao, Y. Cancer statistics, 2008. CA. Cancer J. Clin. 58, 71–96 (2008).

9. Kester, R. T., Bedard, N., Gao, L. & Tkaczyk, T. S. Real-time snapshot hyperspectral imaging endoscope. J. Biomed. Opt. 16, 056005–056005 (2011).

10. Machida H, Sano Y, Hamamoto Y, Muto M, Kozu, T, Tajiri H and Yoshida S. Narrow-band imaging in the diagnosis of colorectal mucosal lesions: a pilot study. Endoscopy 36, 1094–1098 (2004).

11. Matsumoto T, Esaki M, Fujisawa R, Nakamura S, Yao T, Iida M. Chromoendoscopy, narrow-band imaging colonoscopy, and autofluorescence colonoscopy for detection of diminutive colorectal neoplasia in familial adenomatous polyposis. Dis. Colon Rectum 52, 1160–1165 (2009).

12. McGill SK, Evangelou E, Ioannidis JP, Soetikno RM, Kaltenbach T. Narrow band imaging to differentiate neoplastic and non-neoplastic colorectal polyps in real time: a meta-analysis of diagnostic operating characteristics. Gut. 62(12), 1704-1713 (2012).

13. Miller J.C. Magnetic Resonance Spectroscopy in the Brain. Radiology Rounds. 10(7), 1-6 (2012).

14. Moriichi K, Fujiya M, Sato R, Watari J, Nomura Y, Nata T, Ueno N, Maeda S, Kashima S, Itabashi K, Ishikawa C, Inaba Y, Ito T, Okamoto K, Tanabe H,Mizukami Y, Saitoh Y, Kohgo Y. Back-to-back comparison of auto-fluorescence imaging (AFI) versus high resolution white light colonoscopy for adenoma detection. BMC Gastroenterol. 22;12, 75 (2012).

15. O'Connell J.B, Maggard M.A and Ko C.Y. Colon Cancer Survival Rates With the New American Joint Committee on Cancer Sixth Edition Staging. JNCI J Natl Cancer Inst 96(19), 1420-1425. (2004).

16. Rembacken, B. Rembacken B J, Fujii T, Cairns A, Dixon M F, Yoshida S, Chalmers DM, Axon A T. Flat and depressed colonic neoplasms: a prospective study of 1000 colonoscopies in the UK. The Lancet 355, 1211–1214 (2000).

17. Rex, D. K. Maximizing detection of adenomas and cancers during colonoscopy. Am. J. Gastroenterol. 101, 2866–2877 (2006).

18. Rex D K, Cutler C S, Lemmel G T, Rahmani E Y, Clark D W, Helper D J, Lehman G A, and Mark D G. Colonoscopic miss rates of adenomas determined by back-to-back colonoscopies. Gastroenterol. 112, 24–28 (1997).

19. Saitoh Y, Waxman I, West A B, Popnikolov N K, Gatalica Z, Watari J, Obara T, Kohgo Y, and Pasricha P J. Prevalence and distinctive biologic features of flat colorectal adenomas in a North American population. Gastroenterol. 120, 1657–1665 (2001).

20. Schoenfeld P, Lipscomb S, Crook J, Dominguez J, Butler J, and Holmes L. Accuracy of polyp detection by gastroenterologists and nurse endoscopists during flexible sigmoidoscopy: a randomized trial. Gastroenterol. 117, 312–318 (1999).

21. Seeff LC, Richards TB, Shapiro JA, Nadel MR, Manninen DL, Given LS, Dong FB, Winges LD, McKenna MT. How many endoscopies are performed for colorectal cancer screening? Results from CDC's survey of endoscopic capacity. Gastroenterol. 127, 1670–1677 (2004).

22. Stanfield C.L, Germann W.J. Principles of Human Physiology 3rd Ed (Pearson Education 2008).

23. Su M.Y, Chen-Ming Hsu, Yu-Pin Ho, Pang-Chi Chen, Chun-Jung Lin and Cheng-Tang Chiu Comparative study of conventional colonoscopy, chromoendoscopy, and narrow-band imaging systems in differential diagnosis of neoplastic and nonneoplastic colonic polyps. Am. J. Gastroenterol. 101, 2711–2716 (2006).

24. Wallace, M. B., Wax, A., Roberts, D. N. & Graf, R. N. Reflectance spectroscopy. *Gastrointestinal endoscopy clinics of North America* 19, 233–242 (2009).

25. Leavesley, S.J., N. Annamdevula, J. Boni, S. Stocker, K. Grant, B. Troyanovsky, T.C. Rich, and D.F. Alvarez. "Hyperspectral Imaging Microscopy for Identification and Quantitative Analysis of Fluorescently-Labeled Cells in Highly Autofluorescent Tissue." *Journal of Biophotonics* 5, no. 1 (2012), 67–84. doi:10.1002/jbio.201100066